ACS APPLIED MATERIALS & INTERFACES

Research Article

www.acsami.org

Optimization of Organotin Polymers for Dielectric Applications

Gregory M. Treich,[†,⊥] Shamima Nasreen,[†,‡,⊥] Arun Mannodi Kanakkithodi,[§] Rui Ma,[†] Mattewos Tefferi,[∥] James Flynn,[†] Yang Cao,[∥] Rampi Ramprasad,[§] and Gregory A. Sotzing*[,†]

[†]Polymer Program, University of Connecticut, 97 North Eagleville Road, Storrs, Connecticut 06269, United States

[‡]Department of Chemistry, University of Connecticut, 55 North Eagleville Road, Storrs, Connecticut 06269, United States

[§]Department of Materials Science and Engineering, University of Connecticut, 97 North Eagleville Road, Storrs, Connecticut 06269, United States

[∥]Department of Electrical and Computer Engineering, University of Connecticut, 97 North Eagleville Road, Storrs, Connecticut 06269, United States

Supporting Information

ABSTRACT: Recently, there has been a growing interest in developing wide band gap dielectric materials as the next generation insulators for capacitors, photovoltaic devices, and transistors. Organotin polyesters have shown promise as high dielectric constant, low loss, and high band gap materials. Guided by first-principles calculations from density functional theory (DFT), in line with the emerging codesign concept, the polymer poly(dimethyltin 3,3-dimethylglutarate), p(DMTDMG), was identified as a promising candidate for dielectric applications. Blends and copolymers of poly(dimethyltin suberate), p(DMTSub), and p(DMTDMG) were compared using increasing amounts of p(DMTSub) from 10% to 50% to find a balance between electronic properties and film morphology. DFT calculations were used to gain further insight into the structural and electronic differences between p(DMTSub) and p(DMTDMG). Both blend and copolymer systems showed improved results over the homopolymers with the films having dielectric constants of 6.8 and 6.7 at 10 kHz with losses of 1% and 2% for the blend and copolymer systems, respectively. The energy density of the film measured as a $D-E$ hysteresis loop was 6 J/cc for the copolymer, showing an improvement compared to 4 J/cc for the blend. This improvement is hypothesized to come from a more uniform distribution of diacid repeat units in the copolymer compared to the blend, leading toward improved film quality and subsequently higher energy density.

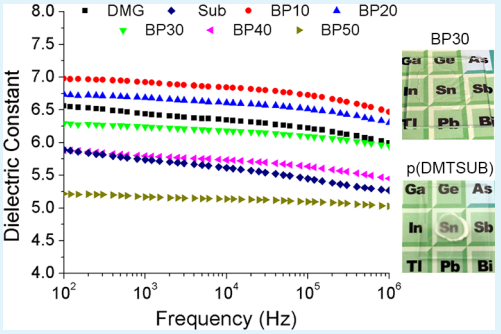

KEYWORDS: *tin, polyester, tin ester, dielectric properties, DFT calculation, structure, thermal properties, breakdown*

1. INTRODUCTION

Dielectric materials have long been important to our lives, with this importance increasing as society progresses toward a more sustainable future from fossil fuels to electrical applications. Solar panels, wind turbines, and other renewable energy sources are driving the demand for energy storage, conversion, and distribution to devices such as electric cars, laptops, and cell phones, which all require advanced dielectric materials. In electronics, there is a consistent drive to produce lighter and smaller components, which can be accomplished, in part, by increasing the dielectric constant of the materials being used.

Polymers have been used as dielectrics due to their ease of processing, allowing them to be formed into flexible films. High dielectric constant and low-loss dielectric polymers are highly desired for advanced electrical applications, such as film capacitors,[1−4] artificial muscles,[5−7] and electrocaloric cooling.[8,9]

For decades, the state-of-the-art polymer dielectric has been biaxially oriented polypropylene (BOPP) because it has an ultralow loss (dissipation factor tan δ of ca. 0.0002) at temperatures up to 85 °C.[10] Above 85 °C, significant dielectric loss from electronic conduction is observed for BOPP.[11] BOPP has a low melting point of approximately 160 °C, allowing it to be easily processed; however, BOPP suffers from a low operational temperature of under 100 °C.[12] BOPP has a dielectric constant of 2.2 and loss on the order of 10^{-4}, which serves as a benchmark to compare all new polymer dielectric materials.[10] Polyvinylidine fluoride (PVDF) is an organic polymer of recent interest in the field of high-energy dielectrics for having a high dielectric constant greater than 10 and a band gap of 6 eV; however, because of the ferroelectric nature of PVDF, a high degree of remnant polarization is observed.[13] By copolymerizing PVDF with bulky groups, random copolymers of P(VDF-CTFE) or P(VDF-HFP) show improved energy densities at upward of 15 J/cc at approximately 600 MV/m.[14,15] Recently, a terpolymer of PVDF, p(VDF-TrFE-CTFE), has been shown to have a dielectric constant of approximately 77 at

Received: April 6, 2016
Accepted: July 28, 2016

DOI: 10.1021/acsami.6b04091
ACS Appl. Mater. Interfaces XXXX, XXX, XXX−XXX

1 kHz through numerous sequential processing methods to fine-tune the morphology.[16] Other organic polymers, such as polyimides, are currently being studied for use as high-temperature dielectric materials.[17,18] Novel and new aromatic polythioureas, polyurethanes, and polyureas have also been investigated recently for high dielectric constant and high breakdown dielectric applications with low loss.[17−23]

The processable nature and lightweight benefits of polymer films come with the drawback of a much lower dielectric constant (ca. 4) than that of inorganics due to a low contribution from the ionic component of the dielectric constant.[24] Inorganic ceramics have been used as capacitor dielectric materials with impressively high dielectric constants, often exceeding 1000, although their relatively high loss, nongraceful failure mode, and low breakdown strength have limited them mostly for low-voltage decoupling applications.[25,26] Barium titanate has long been of interest in the field with dielectric constants over 5000 depending on morphology.[27] These high values are highly sought after by polymer scientists who hope to combine the high dielectric constant with the graceful failure associated with organic films.[28−30] One method that has been attempted to raise the ionic portion of the dielectric constant is the incorporation of inorganic nanoparticles, such as barium titanate, which is accomplished by dispersing such nanoparticles in a polymer.[31] This causes interfacial polarization to occur between the polymer and the barium titanate nanoparticle, increasing the overall dielectric constant for the material.[30,32] In general, without a perfect dispersion of nanoparticles, such an approach is hindered by the sharp dielectric contrast between the high permittivity inorganic nanoparticle and the polymer matrix. This contrast not only allows limited field penetration into the inorganic phase for polarization but also leads to lowered breakdown strength in the polymer matrix due to field concentration. Recent progress has been made in this field using $BaTiO_3$ nanowires with an aspect ratio of 45 to reach dielectric constants up to 44.[33]

Recent studies, both computational and experimental, on aromatic and chiral poly(dimethyltin esters) show a benefit from the incorporation of metal tin atoms in the backbone of a polymer chain through a bond between tin and oxygen.[34−37] This alleviates dispersion difficulties as the tin atoms are dispersed throughout the polymer and unable to aggregate together and drop out of the polymer as nanoparticles can. The ester linkage to the tin atom is an ideal way to bind the metal into the polymer backbone as it provides an increased atomic polarization and can further increase dipole interactions. By varying the length of methylene groups between diacid monomers, aliphatic poly(dimethyltin esters) were able to be produced with different weight percentages of tin.[38,39] During the study on aliphatic poly(dimethyltin esters), a suggestion was made that film morphology based on methylene spacer length was responsible for variations in the dielectric constant and the band gap. The regularly repeating and polar nature of these poly(dimethyltin esters) allowed for high degrees of crystallinity in the polymer powders and films.

In this study, poly(dimethyltin suberate), p(DMTSub), was chosen for further investigation as it had the highest reported band gap of the aliphatic organotin polyesters coupled with a large dielectric constant. A second (and previously not investigated) organotin polyester, poly(dimethyltin 3,3-dimethylglutarate), p(DMTDMG), was studied alongside p(DMTSub).[39] p(DMTDMG) was chosen through a codesign process using DFT calculations to intentionally disrupt large-scale interchain networks that have been predicted and experimentally confirmed by IR spectroscopy.[40] Guided by first-principles calculations from density functional theory (DFT), we were able to determine structure−property relationships between p(DMTSub) and p(DMTDMG) and offer insights into their hybrid structures. By blending these poly(dimethyltin esters) together and synthesizing copolymers out of them, high dielectric constants can be maintained while controlling morphology and allowing for the formation of homogeneous films. The goal of this work was to determine if blends or copolymers would be more advantageous from a properties perspective and to enable amorphous films to be cast for high-field characterization. From a commercial mindset, copolymers would be preferred, since the extra steps of separate synthesis, purification, and blending are removed.

2. EXPERIMENTAL SECTION

2.1. Materials. Suberic acid (99%) and 3,3-dimethylglutaric acid (98%) were procured from Acros Organic. Certified ACS sodium hydroxide pellets (97%) were purchased from Fisher Scientific. Dimethyltin dichloride (98%) was procured from TCI America, and HPLC-grade tetrahydrofuran (THF) was from J.T. Baker. Deionized water was collected from a Millipore Super-Q purification system. All chemicals were used as received with no further purification.

2.2. Synthesis Methodology. Scheme 1 shows the general reaction procedure for the synthesis of tin polyesters as homopolymers and copolymers. For the homopolymer synthesis, 0.015 mol of diacid and 0.032 mol of sodium hydroxide (NaOH) were added and dissolved in a 100 mL round-bottom flask filled with 20.0 mL of deionized water equipped with a magnetic stir bar. In a second flask, 0.015 mol of dimethyl tin dichloride was dissolved in 18.0 mL of THF. The THF solution was then added to the aqueous solution and allowed to polymerize at approximately 20 °C until the polymer precipitated from the solution. The precipitate was then filtered and washed with three 50.0 mL portions of a 1:1 mixture of water and THF and dried in vacuo (30 in. Hg) at 115 °C for 24 h.

Scheme 1. Polymerization Reaction Scheme of Homopolymers and Copolymers of 3,3-Dimethylglutaric Acid and/or with Suberic Scid

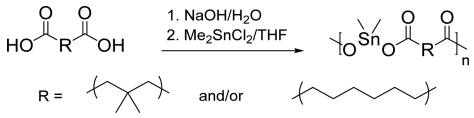

Scheme 1 also represents the general scheme for copolymer synthesis. For example, the following procedure was adopted for the synthesis of poly[(dimethyltin suberate)-*co*-(dimethyltin 3,3-dimethylglutarate)] with 50% of the diacid being suberic acid and the remaining 3,3-dimethylglutaric acid. For simplicity, the polymer will henceforth be referred to as CP50 with the 50 referring to 50% suberic acid, and subsequent polymers will have similar nomenclature. For CP50, 0.0075 mol of suberic acid (1.3065 g) and 0.0075 mol of 3,3-dimethylglutaric acid (1.2013 g) with 0.032 mol of sodium hydroxide (1.2800 g) were dissolved in a round-bottom flask with 20.0 mL of deionized water equipped with a magnetic stir bar. To a second flask, 0.015 mol of dimethyl tin dichloride (3.2954 g) was added and dissolved in 18.0 mL of THF. The THF solution was then added to the aqueous solution, and polymerization was carried out at approximately 20 °C until the polymer precipitated from the solution. The precipitate was then filtered and washed with three 50 mL portions of a 1:1 mixture of water and THF and dried in vacuo (30 in. Hg) at 115 °C for 24 h. The other copolymers were named CP10, CP20, CP30, and CP40 containing 10%, 20%, 30% and 40% of the

DOI: 10.1021/acsami.6b04091
ACS Appl. Mater. Interfaces XXXX, XXX, XXX−XXX

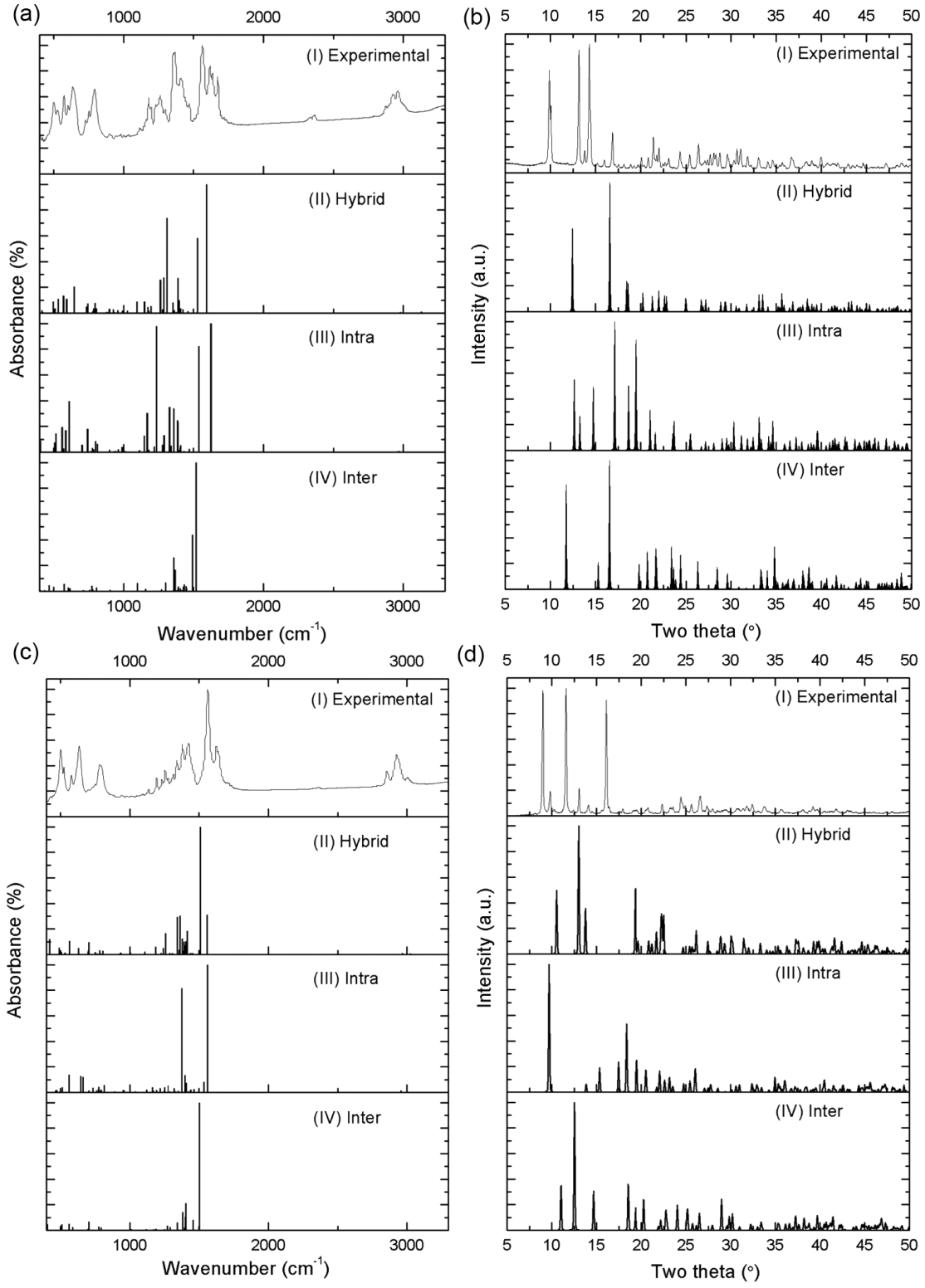

Figure 1. Comparison of p(DMTDMG) (a) FTIR and (b) powder XRD spectra alongside p(DMTSub) (c) FTIR and (d) powder XRD spectra. DFT results for the three different motifs are compared beneath the experimental results.

suberic acid moiety, respectively, with the corresponding amount of 3,3-dimethylglutaric acid.

Blends were prepared as a 10 wt/wt % of total polymer to total solution in m-cresol solvent by mixing p(DMGSub) and p(DMTDMG) homopolymers with varying mass ratios from 10% to 50% at approximately 20 °C. Different blends were named BP10, BP20, BP30, BP40, and BP50 containing 10%, 20%, 30%, 40%, and 50% of p(DMTSub), respectively, with the remainder being p(DMTDMG).

2.3. Film Processing. Copolymer solutions of 10 wt/wt % of total polymer to total solution in m-cresol were prepared for film casting. Blends and copolymers were filtered with 0.45 μm syringe filters and drop casted onto 1 in. 302 stainless steel shim stock discs (McMaster-Carr) for dielectric measurements, uncoated glass microscope slides

DOI: 10.1021/acsami.6b04091
ACS Appl. Mater. Interfaces XXXX, XXX, XXX−XXX

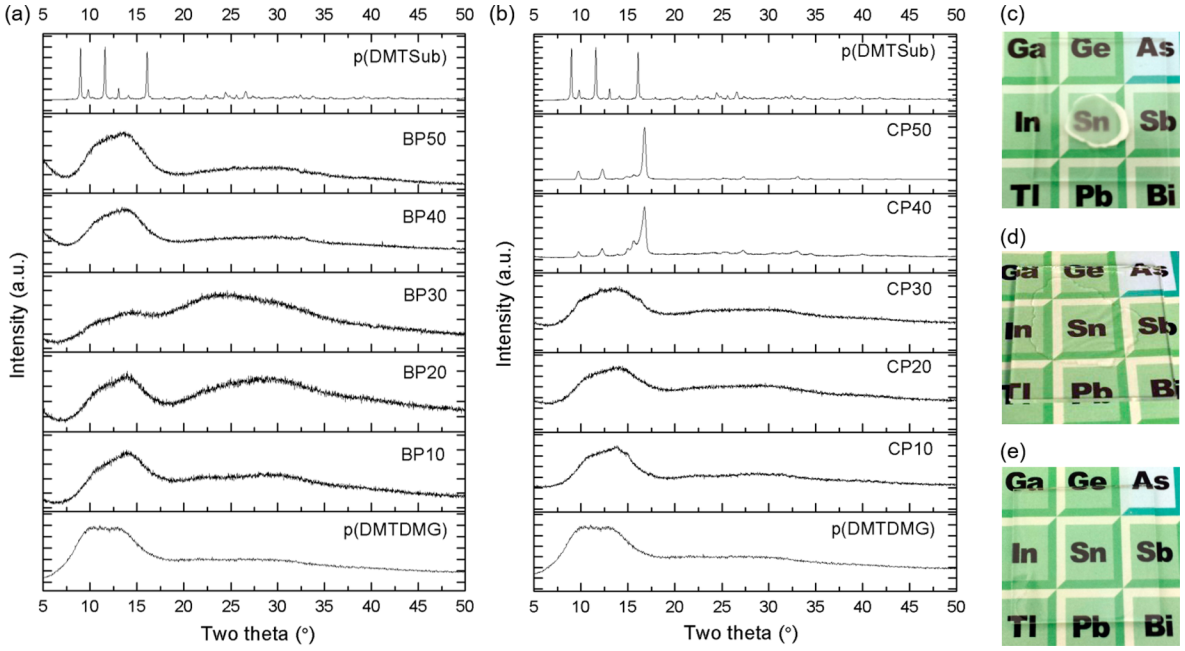

Figure 2. Comparison of tin polyester blends cast on microscope slides: (a) film XRD spectra of blends; (b) film XRD spectra of copolymers; (c) p(DMTSub); (d) BP30; (e) p(DMTDMG).

(Fisher Scientific) for X-ray diffraction (XRD) analysis, and quartz microscope slides (Fisher Scientific) for band gap measurement. The blended solutions were dried on a leveled hot plate for 1 h at 100 °C in a fume hood to evaporate the solvent. The films were then dried in vacuo (30 in. Hg) for 24 h at 150 °C and then cooled to approximately 20 °C.

2.4. Characterization Techniques. Characterization was carried out on vacuum-dried films as detailed above, and the film thickness was determined using a Measure It All LE1000-2 m with several points measured in the testing location and averaged together. Fourier transform infrared (FTIR) spectra were collected on powder samples using a Nicolet Magna 560 FTIR spectrometer with a Specac Quest Diamond attenuated total reflectance (ATR) accessory (resolution 0.35 cm^{-1}) and are reported in wavenumbers (cm^{-1}). Thermogravimetric analysis (TGA) was performed using a TA Instruments TGA Q500 with a heating rate of 10 °C min^{-1} under nitrogen atmosphere. Differential scanning calorimetry (DSC) was performed on a TA Instruments DSC Q20 under nitrogen atmosphere with aluminum pans. An initial heating cycle rate of 40 °C min^{-1} followed by a cooling cycle of 40 °C min^{-1} was used to remove the thermal history; then, a second heating cycle of 10 °C min^{-1} was used to investigate glass and melt transitions. XRD patterns were collected on a Bruker D2 phaser with a Cu Kα (λ = 1.54184 Å) source beam. Dielectric spectroscopy was performed in ambient atmosphere on an Agilent 4284A Precision LCR meter sweeping from 100 Hz to 1 MHz at 25 °C in between two guarded silicone electrodes with an area of 0.78 cm^2. Optical band gap measurements were taken by scanning the UV−visible spectrum from 800 to 200 nm and measuring the wavelength of absorption onset. Polarization measurements were conducted with a modified Sawyer−Tower circuit, employing a Trek Model 10/40 10 kV high-voltage amplifier and an OPA541 operational amplifier-based current to voltage converter.

2.5. Calculation Methodology. The low-energy crystal structural arrangements of p(DMTSub) and p(DMTDMG) were determined using DFT[41] as the computational tool. DFT was applied as implemented in the Vienna ab initio simulation package[42] using the Perdew, Burke, and Ernzerhof functional[43] bolstered with the DFT-DF2 vdW correction[44,45] to explicitly take the weak interactions between polymer chains into account. Given that prior knowledge of the ground-state crystal structures of such Sn ester based polymers is not available, the minima hopping algorithm[46] was used to explore different configurations of the respective polymer repeat units for p(DMTSub) and p(DMTDMG). On the basis of the energies computed using DFT, we obtained three kinds of structural motifs for each polymer that constitute the "global minima" in energy with respect to the configurational space under consideration. These motifs, as noted in Figure 1 and explained in detail by Baldwin et al.,[38,39] are the intra, inter, and hybrid motifs, differing from one another in terms of the extent of cross-linking between adjoining polymer chains. Once these structures were obtained, density functional perturbation theory (DFPT)[47] was employed to calculate their respective dielectric constants. In each computation, dielectric tensors were obtained, and the reported dielectric constant values are the traces of these tensors. Further, the band gaps were computed for all the predicted structures using hybrid electron exchange-correlation functionals,[48] which are known to correct for the underestimation that comes from standard DFT.[49] The XRD patterns and IR spectra for the ground-state polymer structures were computed for a direct comparison with the respective experimentally obtained patterns and spectra. The XRD intensities were given by the square of the structure factor modulus, which depends on reciprocal lattice vectors of the given structure.[50] The IR intensities for different frequency modes were calculated utilizing the same DFPT computations for dielectric constants and were given as a function of Born effective charge tensors and phonon mode eigenvectors for all the atoms in the system.[51]

3. RESULTS AND DISCUSSION

3.1. Rational Selection of Materials. Previous studies on poly(dimethyltin glutarate), p(DMTGlu), showed a material with a dielectric constant of approximately 6.2 and a band gap of approximately 4.7 eV; however, interchain coordination produced large networks of polymer chains that resulted in poor film quality.[38] These films were inadequate for sensitive high-field measurements, which are used to determine dielectric linearity and energy density. DFT enabled quick screening of a number of potential replacements, and p(DMTDMG) was shown to have a similar calculated dielectric constant and a high band gap of 6.1 eV, along with an increase in free volume and steric hindrance. While p(DMTDMG) also had trouble forming films, blending it with 20% p(DMTGlu) produced

DOI: 10.1021/acsami.6b04091
ACS Appl. Mater. Interfaces XXXX, XXX, XXX−XXX

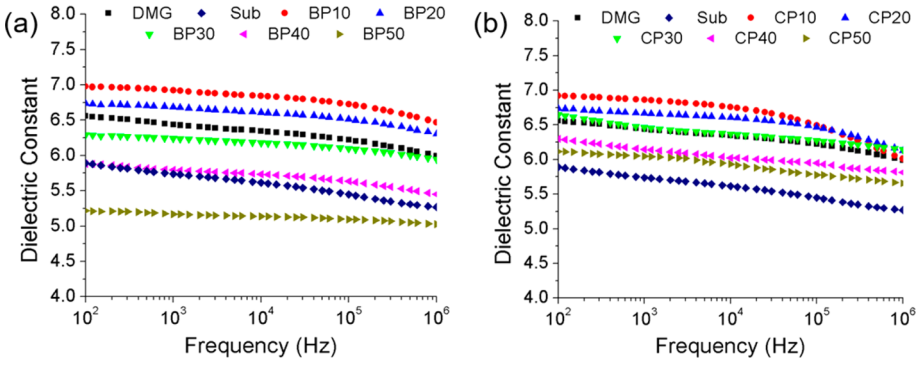

Figure 3. Dielectric constants for tin polyester homopolymers and (a) blends or (b) copolymers at 25 °C open to ambient atmosphere.

Table 1. Dielectric Constant and Loss Values Taken at 10 kHz for Tin Polyesters and Their Band Gaps[a]

polymer	p(DMTSub)	p(DMTDMG)	BP10	BP20	BP30	BP40	BP50	CP10	CP20	CP30	CP40	CP50
dielectric constant (10 kHz)	5.6 (5.5)	6.3 (5.3)	6.8	6.6	6.2	5.7	5.1	6.7	6.6	6.4	6.0	5.9
loss (10 kHz)	1.7	1.2	0.9	0.8	0.7	0.9	0.5	1.8	1.0	1.0	1.4	1.8
optical band gap (eV)	6.7 (6.2)	4.8 (5.9)	4.8	4.8	4.8	4.8	4.8	4.8	4.9	4.9	4.9	4.9

[a]DFT results shown in parentheses are material predictions, calculated from the average of the three structural motifs labeled as inter, intra, and hybrid.

films suitable for *D*−*E* hysteresis loops. For this study, p(DMTSub) was chosen over p(DMTGlu), since it was shown to have a higher band gap (6.7) and dielectric constant (6.6) as a pressed powder pellet.[39]

3.2. Structural Characterization. Figure 1 represents the structural characterization of p(DMTDMG) showing both experimental and computational manifestation alongside the previously studied p(DMTSub).[39] FTIR spectroscopy was used to examine the presence of three different motifs—inter, intra, and hybrid—found in tin polyesters as previously speculated by Peruzzo et al.,[52] reported by Carraher,[53] and confirmed by Baldwin et al.[37−39] The important Sn−O mode here was the tin carboxylate seen in the range 630−643 cm^{-1}. For C−O, the modes of interest were asymmetric bridging and nonbridging bonds, which occurred at 1550−1580 and 1635−1660 cm^{-1}, respectively[54−56] Symmetric bridging and nonbridging occurred at 1410−1430 and 1350−1370 cm^{-1}, respectively, resembling the calculated spectra for p(DMTDMG) and p(DMTSub) in Figure 1a and c, respectively.[54−56] The powder XRD patterns showed these bonds against the computationally predicted spectra of the three competing motifs to compliment the FTIR data. The XRD patterns for the homopolymers p(DMTDMG) and p(DMTSub) in Figure 1b and d, respectively, do not contain exact peak resemblance for any of the three motifs: inter, intra, and hybrid. DFT predictions use the lowest energy structures found for each of the three motifs; however, lower energy structures could exist that were not found by the minima hopping algorithm. In addition, more complex motifs could form besides the three considered here containing many variations of inter and intra motifs along the polymer backbone. These motifs would manifest themselves with different diffraction patterns and could be represented in the experimental diffraction pattern. Considering these complex motifs would make the DFT calculations impractical, and no predictions are able to be made on their FTIR spectra, XRD patterns, or electronic properties.

All films were casted on glass microscope slides, as described in Section 2.3, while dried powders were placed in a clean sample holder and analyzed on a Bruker D2 phaser. The stacked XRD patterns are plotted in Figure 2a showing changes as the p(DMTSub) weight percent increases from bottom to top, resulting in an amorphous nature of all blends in varying extent. The homopolymer p(DMTSub) film in Figure 2c was found to be semicrystalline in nature and confirmed by the near total absence of an amorphous region in the XRD pattern. The crystalline nature of p(DMTDMG), seen in Figure 1b, disappeared when cast as a film on glass slides from m-cresol. This can be visually observed in Figure 2, in the images of the cast BP30 film (d) as well as the homopolymer p(DMTDMG) film (e).

To further investigate the morphological dependence of these systems, 3,3-dimethylglutaratic acid was copolymerized with suberic acid to disrupt the chain packing and provide a different amorphous nature than the blends. By providing a random distribution of the different diacids throughout the film, an increase in relative permittivity and breakdown strength is expected to occur.[57] Low ratios of suberic acid content in copolymers were also seen to be amorphous under visual inspection and confirmed in the XRD with a broad peak at low angles. As the ratio increased to 40% of suberic acid and above, the films became opaque and were shown to have sharp peaks characteristic of a crystalline structure. The peaks became increasingly similar to that of a p(DMTSub) homopolymer, which was the same for both powder and film. This showed a decreasing effect in the ability of 3,3-dimethylglutaric acid to disrupt chain packing as the concentration of it decreases in the overall copolymer composition. The FTIR spectra were collected for all of the copolymers and analyzed in a similar manner to the homopolymers. The spectral analysis confirmed the presence of the three different motifs for the metal carboxylate bonds. All copolymers were also tested for their onset of degradation via TGA and any thermal transitions via DSC with the procedure described in Section 2.4. Degradation occurred around 250 °C for all copolymers, displaying no thermal transitions in the region before degradation. All FTIR, TGA, and DSC plots are enclosed in the Supporting Information.

DOI: 10.1021/acsami.6b04091
ACS Appl. Mater. Interfaces XXXX, XXX, XXX−XXX

3.3. Dielectric Properties. Dielectric spectroscopy was carried out for all the blend and copolymer films. The results for the dielectric constants for the blends and copolymers plotted against frequency are shown in Figure 3a and b, respectively, along with p(DMTDMG) and p(DMTSub) for comparison. Dielectric spectroscopy results in Figure 3a showed the effect of blending homopolymers on improving the dielectric constant of the overall film. BP50 showed the lowest dielectric constant of 5.1 at 10 kHz. Decreasing the concentration of p(DMTSub) to 40%, BP40, brought the dielectric constant up to 5.7, which is similar to the value for pure p(DMTSub). Further decreasing to 30% p(DMTSub), BP30, brought the dielectric constant to 6.2, which is in the same range as the dielectric constant of p(DMTDMG) at 6.3. A subsequent decrease of p(DMTSub) content in the blend brought the dielectric constant higher than the homopolymers to a value of 6.8 for BP10 and 6.6 for BP20 at 10 kHz. The loss values around 10 kHz are shown in Table 1 and were all below 1% for the blends, which is acceptable for many energy storage applications.

The dielectric constants for copolymers, as seen in Figure 3b, were shown to increase as the amount of suberic acid was decreased and replaced with 3,3-dimethylglutaric acid, which could be correlated with a decrease in crystallinity. The two highest dielectric constants were found to be for CP10 at 6.7 and CP20 at 6.6 at 10 kHz. The loss values of copolymer films were slightly higher than those of the films of blends as seen in Table 1; still, all of the copolymers had less than 2% loss with the highest value for CP50 at 1.8% loss and the lowest being CP20 at 1% loss.

3.4. Breakdown Strength and Band Gap. Insulating polymers exceed their breakdown field when electrons from the valence band are promoted to the conduction band to an extent that creates an electron avalanche.[58] The energy gap between the valence band and the conduction band, or the band gap, can be used as an indicator for intrinsic breakdown strength; a larger band gap would allow a higher field before breakdown.[59] As previously reported, the band gap of the p(DMTSub) homopolymer was the largest among aliphatic p(dimethyltin esters) at 6.5 eV, and the band gap of p(DMTDMG) was experimentally determined to be at 4.8 eV.[39] The calculated value for the p(DMTSub) band gap shows close agreement with experiments compared to p(DMTDMG) as seen in Table 1, where the predicted values from DFT are shown in parentheses. This result is expected as p(DMTSub), which is more crystalline than p(DMTDMG), closely resembles the morphology used for band gap calculations. As determined by UV absorption, the band gaps of polymer blends corresponded to the lowest band gap component, p(DMTDMG), which has a band gap of 4.8 eV. This value is above the criteria previously set forth, that is, that a band gap greater than 3 eV would lead to high breakdown strengths.[21] Similarly, all of the copolymers studied were found to have a band gap close to p(DMTDMG), and the band gap values are between 4.8 and 4.9 eV. A band gap of approximately 5 eV should give a high intrinsic breakdown; however, experimental issues such as impurities arising from trapped solvent and structural defects due to them may lower the measured breakdown.[60] More importantly, 3,3-dimethylglutaric acid has proven essential in allowing tin polyester films to be made with sufficient quality that such measurements can be taken.

3.5. Polarization Measurements. The first *D*−*E* hysteresis loops reported for tin polyester polymers were performed on p(DMTGlu),[38] which was blended with 80% by weight p(DMTDMG) to give a suitable film for analysis.[38] A *D*−*E* loop was also reported for BP20.[39] To give a direct comparison between the previously studied blends, we reported the *D*−*E* hysteresis loop for the copolymer system CP20 as shown in Figure 4. The films were prepared as described by Baldwin et al.

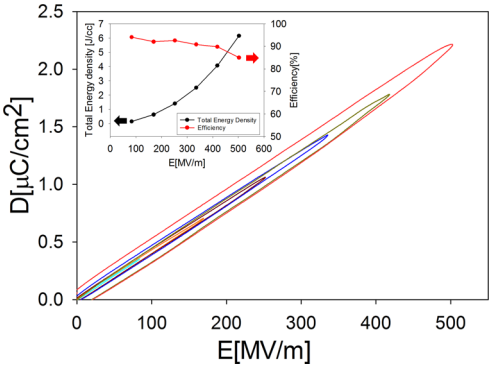

Figure 4. *D*−*E* hysteresis loop for CP20 along with an inset showing the corresponding total energy density and efficiency plot.

where a 0.07 cm^2 section of the film was metalized by sputtering a Au/Pd (80/20 wt %) electrode.[38] Breakdown for CP20 was observed at approximately 500 MV/m with a maximum energy density of approximately 6 J/cc. This is an increase over BP20 that was found to have breakdown of approximately 300 MV/m with an energy density of approximately 4 J/cc and the p(DMTGlu) blend that had a breakdown of approximately 400 MV/m and an energy density of approximately 4 J/cc.[38,39] The efficiency remained above 90% until the electric field reached the limit of the material, 500 MV/m, after which the efficiency dropped to 85%. The improved breakdown and energy density measurements for the copolymer over the blends are attributed to improved film formation and uniformity. For polar polymers, it has been proposed that random dipoles in the amorphous region contribute electron-dipole scattering to prevent dielectric breakdown by stabilizing electron energy.[57] Blends have the ability to phase separate into small domains, but the copolymers force the bulky 3,3-dimethyl group in close proximity to the suberate group to suppress crystallinity.

4. CONCLUSION

In summary, in keeping with the emerging codesign concept in which computational and experimental work are synergistically employed, we have shown how computational guidance by DFT enabled the selection of a complementary polymer, p(DMTDMG), which allowed high-field characterization of previously studied aliphatic tin polyesters through blending and copolymerization. By introducing the 3,3-dimethylglutarate unit into poly(dimethyltin esters), the degradation of film quality due to crystallinity has been reduced while the dielectric constant and energy density have been improved. This goes against the trend for nonpolar polymers, most notably BOPP, where biaxially stretching to increase crystallinity also increases the breakdown field to approximately 700 MV/m. Through further use of DFT calculations, the homopolymers p(DMTSub) and p(DMTDMG) were studied in depth with predicted IR spectra, XRD spectra, band gaps, and dielectric constants closely matching experimental results. Films made from the blend BP20 and copolymer CP20 both showed high

DOI: 10.1021/acsami.6b04091
ACS Appl. Mater. Interfaces XXXX, XXX, XXX−XXX

dielectric constants of 6.6 and loss of approximately 1%. Copolymerization was found to be better suited than blending for energy storage as the energy density of CP20 was calculated at approximately 6 J/cc compared to 4 J/cc for BP20. The insights from this research will help to improve the feasibility of poly(dimethyltin esters) for use as a next generation polymer dielectric.

■ ASSOCIATED CONTENT

Supporting Information

The Supporting Information is available free of charge on the ACS Publications website at DOI: 10.1021/acsami.6b04091.

Detailed synthetic information for both the homopolymers and copolymers; FTIR and UV−visible spectra; TGA and DSC analyses; and computational data (PDF)

■ AUTHOR INFORMATION

Corresponding Author

* Email: g.sotzing@uconn.edu.

Author Contributions

⊥G.M.T. and S.N. contributed equally to this work. All authors have given approval to the final version of the manuscript.

Notes

The authors declare no competing financial interest.

■ ACKNOWLEDGMENTS

This work is supported through a multidisciplinary university research initiative (MURI) grant through the Office of Naval Research (N00014-10-1-0944). The authors would like to acknowledge JoAnne Ronzello for valuable insight and for assisting in dielectric measurements.

■ REFERENCES

(1) Chen, Q.; Shen, Y.; Zhang, S.; Zhang, Q. M. Polymer-Based Dielectrics with High Energy Storage Density. *Annu. Rev. Mater. Res.* **2015**, *45* (1), 433−458.

(2) Zhu, L.; Wang, Q. Novel Ferroelectric Polymers for High Energy Density and Low Loss Dielectrics. *Macromolecules* **2012**, *45* (7), 2937−2954.

(3) Sarjeant, W. J.; Zirnheld, J.; MacDougall, F. W. Capacitors. *IEEE Trans. Plasma Sci.* **1998**, *26* (5), 1368−1392.

(4) Sarjeant, W. J.; Clelland, I. W.; Price, R. A. Capacitive Components for Power Electronics. *Proc. IEEE* **2001**, *89* (6), 846−855.

(5) Brochu, P.; Pei, Q. Advances in Dielectric Elastomers for Actuators and Artificial Muscles. *Macromol. Rapid Commun.* **2010**, *31* (1), 10−36.

(6) Federico, C.; De Rossi, D.; Kornbluh, R.; Pelrine, R.; Sommer-Larsen, P. *Dielectric Elastomers as Electromechanical Transducers: Fundamentals, Materials, Devices, Models and Applications of an Emerging Electroactive Polymer Technology*; Elsevier Science: Boston, MA, 2008; pp 301−313.

(7) Pelrine, R.; Kornbluh, R.; Joseph, J.; Heydt, R.; Pei, Q.; Chiba, S. High-Field Deformation of Elastomeric Dielectrics for Actuators. *Mater. Sci. Eng., C* **2000**, *11* (2), 89−100.

(8) Lu, S.-G.; Zhang, Q. Electrocaloric Materials for Solid-State Refrigeration. *Adv. Mater.* **2009**, *21* (19), 1983−1987.

(9) Neese, B.; Chu, B.; Lu, S.-G.; Wang, Y.; Furman, E.; Zhang, Q. M. Large Electrocaloric Effect in Ferroelectric Polymers Near Room Temperature. *Science (Washington, DC, U. S.)* **2008**, *321* (5890), 821−823.

(10) Ho, J.; Jow, R. *Characterization of High Temperature Polymer Thin Films for Power Conditioning Capacitors*; ARL-TR- 4880; Army Research Laboratories: Adelphi, MD, 2009.

(11) Ho, J.; Jow, T. R. High Field Conduction in Biaxially Oriented Polypropylene at Elevated Temperature. *IEEE Trans. Dielectr. Electr. Insul.* **2012**, *19* (3), 990−995.

(12) Longo, C.; Savaris, M.; Zeni, M.; Brandalise, R. N.; Grisa, A. M. C. Degradation Study of Polypropylene (PP) and Bioriented Polypropylene (BOPP) in the Environment. *Mater. Res.* **2011**, *14* (4), 442−448.

(13) Chu, B.; Zhou, X.; Ren, K.; Neese, B.; Lin, M.; Wang, Q.; Bauer, F.; Zhang, Q. M. A Dielectric Polymer with High Electric Energy Density and Fast Discharge Speed. *Science (Washington, DC, U. S.)* **2006**, *313* (5785), 334−336.

(14) Guan, F.; Pan, J.; Wang, J.; Wang, Q.; Zhu, L. Crystal Orientation Effect on Electric Energy Storage in Poly(vinylidene Fluoride-Co-Hexafluoropropylene) Copolymers. *Macromolecules* **2010**, *43* (1), 384−392.

(15) Zhou, X.; Chu, B.; Neese, B.; Lin, M.; Zhang, Q. M. Electrical Energy Density and Discharge Characteristics of A Poly(vinylidene Fluoridechlorotrifluoroethylene) Copolymer. *IEEE Trans. Dielectr. Electr. Insul.* **2007**, *14*, 1133−1138.

(16) Smith, O. L.; Kim, Y.; Kathaperumal, M.; Gadinski, M. R.; Pan, M. J.; Wang, Q.; Perry, J. W. Enhanced Permittivity and Energy Density in Neat Poly(vinylidene Fluoride-Trifluoroethylene-Chlorotrifluoroethylene) Terpolymer Films through Control of Morphology. *ACS Appl. Mater. Interfaces* **2014**, *6* (12), 9584−9589.

(17) Ma, R.; Baldwin, A. F.; Wang, C.; Offenbach, I.; Cakmak, M.; Ramprasad, R.; Sotzing, G. A. Rationally Designed Polyimides for High-Energy Density Capacitor Applications. *ACS Appl. Mater. Interfaces* **2014**, *6* (13), 10445−10451.

(18) Baldwin, A. F.; Ma, R.; Wang, C.; Ramprasad, R.; Sotzing, G. A. Structure-Property Relationship of Polyimides Based on Pyromellitic Dianhydride and Short-Chain Aliphatic Diamines for Dielectric Material Applications. *J. Appl. Polym. Sci.* **2013**, *130* (2), 1276−1280.

(19) Lorenzini, R. G.; Kline, W. M.; Wang, C. C.; Ramprasad, R.; Sotzing, G. A. The Rational Design of Polyurea & Polyurethane Dielectric Materials. *Polymer* **2013**, *54* (14), 3529−3533.

(20) Ma, R.; Sharma, V.; Baldwin, A. F.; Tefferi, M.; Offenbach, I.; Cakmak, M.; Weiss, R.; Cao, Y.; Ramprasad, R.; Sotzing, G.A. Rational Design and Synthesis of Polythioureas as Capacitor Dielectrics. *J. Mater. Chem. A* **2015**, *3* (28), 14845−14852.

(21) Sharma, V.; Wang, C.; Lorenzini, R. G.; Ma, R.; Zhu, Q.; Sinkovits, D. W.; Pilania, G.; Oganov, A. R.; Kumar, S.; Sotzing, G. A.; Boggs, S. A.; Ramprasad, R. Rational Design of All Organic Polymer Dielectrics. *Nat. Commun.* **2014**, *5*, 4845−4852.

(22) Wu, S.; Li, W.; Lin, M.; Burlingame, Q.; Chen, Q.; Payzant, A.; Xiao, K.; Zhang, Q. M. Aromatic Polythiourea Dielectrics with Ultrahigh Breakdown Field Strength, Low Dielectric Loss, and High Electric Energy Density. *Adv. Mater.* **2013**, *25* (12), 1734−1738.

(23) Tefferi, M.; Ma, R.; Treich, G.; Sotzing, G.; Ramprasad, R.; Cao, Y. Novel Dielectric Films with High Energy Density. *Electr. Insul. Dielectr. Phenom. (CEIDP), 2015 IEEE Conf.* **2015**, 451−454.

(24) Wang, C. C.; Pilania, G.; Boggs, S. A.; Kumar, S.; Breneman, C.; Ramprasad, R. Computational Strategies for Polymer Dielectrics Design. *Polymer* **2014**, *55* (4), 979−988.

(25) Sebastian, M. T.; Jantunen, H. Low Loss Dielectric Materials for LTCC Applications: A Review. *Int. Mater. Rev.* **2008**, *53* (2), 57−90.

(26) Tong, S.; Ma, B.; Narayanan, M.; Liu, S.; Koritala, R.; Balachandran, U.; Shi, D. Lead Lanthanum Zirconate Titanate Ceramic Thin Films for Energy Storage. *ACS Appl. Mater. Interfaces* **2013**, *5* (4), 1474−1480.

(27) Arlt, G.; Hennings, D.; De With, G. Dielectric Properties of Fine-Grained Barium Titanate Ceramics. *J. Appl. Phys.* **1985**, *58* (4), 1619−1625.

(28) Rabuffi, M.; Picci, G. Status Quo and Future Prospects for Metallized Polypropylene Energy Storage Capacitors. *IEEE Trans. Plasma Sci.* **2002**, *30* (5), 1939−1942.

(29) Tortai, J. H.; Bonifaci, N.; Denat, A.; Trassy, C. Diagnostic of the Self-Healing of Metallized Polypropylene Film by Modeling of the Broadening Emission Lines of Aluminum Emitted by Plasma Discharge. *J. Appl. Phys.* **2005**, *97* (5), 053304.

(30) Zhu, L. Exploring Strategies for High Dielectric Constant and Low Loss Polymer Dielectrics. *J. Phys. Chem. Lett.* **2014**, *5* (21), 3677−3687.
(31) Thakur, V.; Kessler, M. Polymer Nanocomposites: New Advanced Dielectric Materials for Energy Storage Applications. In *Advanced Energy Materials*; Tiwari, A., Valyukh, S., Eds.; John Wiley & Sons, Inc.: Hoboken, NJ, USA, 2014; pp 207−257.
(32) Riggs, B. C.; Elupula, R.; Rehm, C.; Adireddy, S.; Grayson, S. M.; Chrisey, D. B. Click-In Ferroelectric Nanoparticles for Dielectric Energy Storage. *ACS Appl. Mater. Interfaces* **2015**, *7* (32), 17819−17825.
(33) Tang, H.; Zhou, Z.; Sodano, H. A. Relationship between BaTiO3 Nanowire Aspect Ratio and the Dielectric Permittivity of Nanocomposites. *ACS Appl. Mater. Interfaces* **2014**, *6* (8), 5450−5455.
(34) Mannodi-Kanakkithodi, A.; Wang, C. C.; Ramprasad, R. Compounds Based on Group 14 Elements: Building Blocks for Advanced Insulator Dielectrics Design. *J. Mater. Sci.* **2015**, *50* (2), 801−807.
(35) Van Daal, H. J. The Static Dielectric Constant of SnO2. *J. Appl. Phys.* **1968**, *39* (9), 4467−4469.
(36) Pilania, G.; Wang, C. C.; Wu, K.; Sukumar, N.; Breneman, C.; Sotzing, G.; Ramprasad, R. New Group IV Chemical Motifs for Improved Dielectric Permittivity of Polyethylene. *J. Chem. Inf. Model.* **2013**, *53* (4), 879−886.
(37) Baldwin, A. F.; Ma, R.; Huan, T. D.; Cao, Y.; Ramprasad, R.; Sotzing, G. A. Effect of Incorporating Aromatic and Chiral Groups on the Dielectric Properties of Poly (Dimethyltin Esters). *Macromol. Rapid Commun.* **2014**, *35* (24), 2082−2088.
(38) Baldwin, A. F.; Ma, R.; Mannodi-Kanakkithodi, A.; Huan, T. D.; Wang, C.; Tefferi, M.; Marszalek, J. E.; Cakmak, M.; Cao, Y.; Ramprasad, R.; Sotzing, G. A. Poly(dimethyltin Glutarate) as a Prospective Material for High Dielectric Applications. *Adv. Mater.* **2015**, *27* (2), 346−351.
(39) Baldwin, A. F.; Huan, T. D.; Ma, R.; Mannodi-Kanakkithodi, A.; Tefferi, M.; Katz, N.; Cao, Y.; Ramprasad, R.; Sotzing, G. A. Rational Design of Organotin Polyesters. *Macromolecules* **2015**, *48* (8), 2422−2428.
(40) Mannodi-Kanakkithodi, A.; Treich, G. M.; Huan, T. D.; Ma, R.; Tefferi, M.; Cao, Y.; Sotzing, G. A.; Ramprasad, R. Rational Co-Design of Polymer Dielectrics for Energy Storage. *Adv. Mater.* **2016**, DOI: 10.1002/adma.201600377.
(41) Hohenberg, P.; Kohn, W. Inhomogeneous Electron Gas. *Phys. Rev.* **1964**, *136* (3B), B864−B871.
(42) Kresse, G.; Hafner, J. Ab Initio Molecular Dynamics for Liquid Metals. *Phys. Rev. B: Condens. Matter Mater. Phys.* **1993**, *47* (1), 558−561.
(43) Perdew, J. P.; Burke, K.; Ernzerhof, M. Generalized Gradient Approximation Made Simple. *Phys. Rev. Lett.* **1996**, *77* (18), 3865−3868.
(44) Klimes, J.; Bowler, D. R.; Michaelides, A. Chemical Accuracy for the van Der Waals Density Functional. *J. Phys.: Condens. Matter* **2010**, *22* (2), 022201.
(45) Liu, C. S.; Pilania, G.; Wang, C.; Ramprasad, R. How Critical Are the van Der Waals Interactions in Polymer Crystals? *J. Phys. Chem. A* **2012**, *116* (37), 9347−9352.
(46) Amsler, M.; Botti, S.; Marques, M. A. L.; Goedecker, S. Conducting Boron Sheets Formed by the Reconstruction of the a-Boron (111) Surface. *Phys. Rev. Lett.* **2013**, *111* (13), 1−6.
(47) Baroni, S.; De Gironcoli, S.; Dal Corso, A.; Giannozzi, P. Phonons and Related Crystal Properties from Density-Functional Perturbation Theory. *Rev. Mod. Phys.* **2001**, *73* (2), 515−562.
(48) Heyd, J.; Scuseria, G. E.; Ernzerhof, M. Hybrid Functionals Based on a Screened Coulomb Potential. *J. Chem. Phys.* **2003**, *118* (18), 8207−8215.
(49) Henderson, T. M.; Paier, J.; Scuseria, G. E. Accurate Treatment of Solids with the HSE Screened Hybrid. *Phys. Status Solidi B* **2011**, *248* (4), 767−774.
(50) Roisnel, T.; Rodríquez-Carvajal, J. WinPLOTR: A Windows Tool for Powder Diffraction Pattern Analysis. *Mater. Sci. Forum* **2001**, *378*−*381*, 118−123.
(51) Wang, C. C.; Pilania, G.; Ramprasad, R. Dielectric Properties of Carbon-, Silicon-, and Germanium-Based Polymers: A First-Principles Study. *Phys. Rev. B: Condens. Matter Mater. Phys.* **2013**, *87* (3), 035103.
(52) Peruzzo, V.; Plazzogna, G.; Tagliavini, G. Electrochemical Preparation of Trimethyltin Carboxylates. *J. Organomet. Chem.* **1969**, *18* (1), 89−94.
(53) Carraher, C. E., Jr. Comparative Infrared Spectroscopy of Group IV a Polyesters and Polyoxides. *Angew. Makromol. Chem.* **1973**, *31* (1), 115−122.
(54) Peruzzo, V.; Plazzogna, G.; Tagliavini, G. The Preparation and Properties of Some Allyltin carboxylates:R3SnOOCR′ (R′ = CH3, CH2Cl), R2Sn(OOCR′)2 (R′ = CH2Cl, CHCl2) and [R2Sn-(OOCR′)]2O (R′ = CH2Cl, CHCl2, CCl3). *J. Organomet. Chem.* **1972**, *40* (1), 129−133.
(55) Peruzzo, V.; Plazzogna, G.; Tagliavini, G. The Preparation and Properties of Some Trivinyltin Carboxylates. *J. Organomet. Chem.* **1970**, *24* (2), 347−353.
(56) Plazzogna, G.; Peruzzo, V.; Tagliavini, G. A New Method of Preparing a Soluble Form of Trimethyltin Acetate. *J. Organomet. Chem.* **1969**, *16* (3), 500−502.
(57) Sun, Y.; Boggs, S.; Ramprasad, R. The Effect of Dipole Scattering on Intrinsic Breakdown Strength of Polymers. *IEEE Trans. Dielectr. Electr. Insul.* **2015**, *22* (1), 495−502.
(58) Sun, Y.; Bealing, C.; Boggs, S.; Ramprasad, R. 50+ Years of Intrinsic Breakdown. *IEEE Electr. Insul. Mag.* **2013**, *29* (2), 8−15.
(59) Sun, Y.; Boggs, S. A.; Ramprasad, R. The Intrinsic Electrical Breakdown Strength of Insulators from First Principles. *Appl. Phys. Lett.* **2012**, *101* (13), 132906.
(60) Fothergill, J. C.; Dissoldo, L. A. *Electrical Degradation and Breakdown in Polymers*; Stevens, G. C., Ed.; Peter Peregrinus Ltd.: London, 1992.

DOI: 10.1021/acsami.6b04091
ACS Appl. Mater. Interfaces XXXX, XXX, XXX−XXX